HHS Public Access

Author manuscript

Eur J Neurosci. Author manuscript; available in PMC 2016 January 01.

Published in final edited form as:

Eur J Neurosci. 2015 January ; 41(2): 243–253. doi:10.1111/ejn.12755.

Functional connectivity in the resting-state motor networks influences the kinematic processes during motor sequence learning

Laura Bonzano[1,2], **Eleonora Palmaro**[3], **Roxana Teodorescu**[4], **Lazar Fleysher**[5], **Matilde Inglese**[4,5,6], and **Marco Bove**[3]

[1] Department of Neuroscience, Rehabilitation, Ophthalmology, Genetics, Maternal and Child Health, University of Genoa, Genoa, Italy

[2] Magnetic Resonance Research Centre on Nervous System Diseases, University of Genoa, Genoa, Italy

[3] Department of Experimental Medicine, Section of Human Physiology - University of Genoa, Genoa, Italy

[4] Department of Neurology, Icahn School of Medicine at Mount Sinai New York, NY USA

[5] Department of Radiology, Icahn School of Medicine at Mount Sinai New York, NY USA

[6] Department of Neuroscience - Icahn School of Medicine at Mount Sinai New York, NY USA

Abstract

Neuroimaging studies support the involvement of the cerebello-cortical and striato-cortical motor loops in motor sequence learning. Here, we investigated whether the gain of motor sequence learning could depend on a priori resting-state functional connectivity (rsFC) between **motor areas** and structures belonging to these circuits. Fourteen healthy subjects underwent a resting-state fMRI session. Afterward, they were asked to reproduce a verbally-learned sequence of finger opposition movements as fast and accurate as possible. All subjects increased their movement rate with practice, by reducing touch duration and/or inter tapping interval. The rsFC analysis showed that at rest left and right M1 and left and right supplementary motor cortex (SMA) were mainly connected with other motor areas. The covariate analysis taking into account the different kinematic parameters indicated that the subjects achieving greater movement rate increase were those showing stronger rsFC of the left M1 and SMA with the right lobule VIII of the cerebellum. Notably, the subjects with greater inter tapping interval reduction showed stronger rsFC of the left M1 and SMA with the association nuclei of the thalamus. Conversely, the regression analysis with the right M1 and SMA seeds showed only few significant clusters for the different covariates not located in the cerebellum and thalamus. No common clusters were found between right M1 and SMA. All these findings indicate important functional connections at rest of those neural circuits

Corresponding authors: Dr. Marco Bove, Department of Experimental Medicine, Section of Human Physiology, Viale Benedetto XV 3, 16132, Genoa, Italy Tel: +39 0103538172; Fax: +39 0103538194; marco.bove@unige.it Prof. Matilde Inglese Department of Neurology, Radiology and Neuroscience Director Neurology Imaging Laboratory Icahn School of Medicine at Mount Sinai Annenberg 14, Box 1137, One Gustave L. Levy Place New York, NY 10029 Tel/Fax: 212-824-9310; Fax: 212-348-1310; matilde.inglese@mssm.edu.

responsible of motor learning improvement, involving the motor areas related to the hemisphere directly controlling the finger movements, the thalamus and the cerebellum.

Keywords

Cerebellum; Finger Movement; Learning; Motor **Areas**; Thalamus

Introduction

One of the key aspects of motor learning is the ability to combine sequences of discrete movements into a well articulated, eventually automated behavior (motor sequence learning) (Ashe *et al.*, 2006; Doyon *et al.*, 2009; Moisello *et al.*, 2011). Neuroimaging studies in humans have demonstrated the involvement of the cerebello-cortical and striato-cortical motor loops in the course of motor sequence learning (Doyon & Benali, 2005). Further, some behavioral studies have reported that a number of movement transitions embedded within the motor sequence can differently benefit from practice (Kuriyama *et al.*, 2004; Sheth *et al.*, 2008). In a recent study combining behavior and event-related functional magnetic resonance imaging (fMRI), Orban and colleagues investigated how changes in elementary parameters of single movements may affect the behavioral manifestation and brain mechanisms engaged during the course of finger motor sequence learning (Orban *et al.*, 2011). They demonstrated that partially overlapping and segregated brain networks are associated with the improvement in performance on two distinct kinematic indices: velocity and transition. Specifically, the primary motor cortex (M1) and the anterior spinocerebellum preferentially contribute to performance changes in the velocity of the sequential single movements, whereas the anterior neocerebellum, the putamen, and a larger extent of the frontal motor cortex mediate the improvements in transition that is the time interval between individual movements. The temporal synchronization of neural activity between anatomically separated brain regions is known as functional connectivity (FC) (Aertsen *et al.*, 1989; Friston *et al.*, 1993) and has been investigated by the coherence between brain regions measured on resting-state fMRI (rs-fMRI) time-series (Biswal *et al.*, 1995; Lowe *et al.*, 2000; Xiong *et al.*, 1999). It has been proposed that the resting brain actively and selectively processes previous experiences (Miall & Jackson, 2006), playing a key role in neuronal plasticity. Indeed, it has been shown that a motor learning task can modulate resting-state activity (Albert *et al.*, 2009; Sami & Miall, 2013; Vahdat *et al.*, 2011). In this context, we asked whether the FC of resting-state networks (resting-state functional connectivity - rsFC) related to the cerebello-cortical and striato-cortical motor loops might influence the accomplishment of motor sequence learning and even the adopted strategy, in terms of kinematics processes.

To investigate our hypothesis, a group of healthy subjects was recruited and asked to perform a motor learning task based on a sequence of finger opposition movements immediately after an rsfMRI session. The rsFC analysis was conducted with a “seed voxel” method by using four different seeds: the left and right M1 and the left and right supplementary motor area (SMA), which have been found to be included in the circuits

dealing with velocity and transition processes in motor sequence learning (Orban *et al.*, 2011).

Following the Doyon and Ungerleider's model indicating that the cortico-cerebellum loop is most actively involved in early sequence learning (Doyon *et al.*, 2003), we hypothesized that the gain of motor sequence learning is higher in those subjects showing stronger rsFC between the **motor areas** and the cerebellum, and that separate regions of the cerebellum can be identified as a function of the specific aspect of the motor skill.

Materials and methods

Subjects

Fourteen healthy volunteers (7 females and 7 males; mean age = 30.0 ± 2.4 years), with no history of neurological or psychiatric disorders, were included in this study. All subjects were right-handed and naïve to the purpose of the study; musicians and professional typists were excluded due to preexisting skills requiring highly coordinated finger dexterity. Approval for this study was obtained from the Mount Sinai's Institutional Review Board and informed consent was obtained from all subjects, according to the Declaration of Helsinki.

Dummy task

The whole experimental protocol is shown in Figure 1: every subject underwent a dummy task, a magnetic resonance exam with rs-fMRI, and then was engaged in a motor sequence learning task. At the beginning of the experimental session, immediately before the rs-fMRI scan participants were shown a dummy task lasting 4 min on the computer screen, to ensure a common cognitive baseline in the group (Albert *et al.*, 2009). In details, this task consisted in dynamic point-light displays of human whole-body movements or scrambled versions that showed the same individual dot motions but with random positions (Jastorff *et al.*, 2006). These stimuli lasted 3 s each and were grouped into 30-s interleaved runs of 10 human and 10 scrambled motion stimuli. Subjects were instructed to watch the stimuli trying to discriminate human and scrambled movements, but they had no active task to perform.

Resting-state fMRI acquisition

After the dummy task, and before the motor sequence learning task, subjects underwent brain MRI on a 3.0 Tesla scanner (Philips Achieva, The Netherlands) with an 8-channel SENSE phased-array head coil. The MRI protocol included T2-weighted Turbo Spin Echo sequence (TR/TE = 3000/80 ms; FOV = 230 mm × 230mm; matrix = 512 × 512; slice thickness = 4 mm), 3D T1-weighted Turbo Field Echo sequence (TR/TE/TI = 7.5/3.4/900 ms; voxel size 1×1×1 mm^3). For rs-fMRI, a total of 120 volumes were acquired in a transverse plane using a T2*-weighted echo-planar-imaging sequence (TR/TE = 2607/27 ms; flip angle = 90°; FOV = 210 mm × 210 mm; matrix = 96 × 96; slice thickness = 3 mm; voxel size = 2.19 mm × 2.19 mm × 3 mm). The rs-fMRI settings provided 0.19 Hz bandwidth with 3.5×10^{-3} Hz resolution, which is adequate to select the 0.01-0.1 Hz band of interest (see rs-fMRI analysis below). Each EPI volume included 50 axial slices without gap, covering the entire cerebral cortex and cerebellum. During rs-fMRI, the subjects were

instructed to stay still, with their eyes closed, awake but not engaging in any specific mental activity.

Motor sequence learning task

Immediately after the rs-fMRI session, all participants performed a motor sequence learning task lasting about 30 min. First, subjects were asked to memorize a sequence of numbers using verbal code (3 4 1 3 2 1 4 2) with no actual movement training. This allowed investigating brain mechanisms related to the acquisition of the procedural skill after the declarative skill rather than to the explicit acquisition of the sequence order without superimposing constraints on the motor performance with pacing or cueing signals (Orban *et al.*, 2011). When they were able to repeat the sequence to the experimenter without errors, they were informed about the correspondence of each number with one finger (1, 2, 3 and 4 referred to the index, middle, ring and little fingers, respectively) and were instructed to carry out the eight-element finger motor sequence with their right hand by touching the fingers with the thumb in the correct order, with their eyes closed. Specifically, they were seated in a quiet room and wore a sensor-engineered glove to record the contact between the thumb and another finger (GAS, ETT S.p.A., Italy) (Bove *et al.*, 2007; Moisello *et al.*, 2011). They had to perform the finger motor sequence twice in each trial, as fast and accurately as possible, for a total of 50 practice trials intermingled with rest epochs lasting about 12s.

Resting-state fMRI analysis

The analysis of the rs-fMRI images was conducted by using Data Processing Assistant for Resting-State fMRI (DPARSF), a toolbox developed in MATLAB (MathWorks, Inc.) for pipeline data analysis of rs-fMRI based on some functions included in Statistical Parametric Mapping (SPM) and Resting-State fMRI Data Analysis Toolkit (REST) (Chao-Gan & Yu-Feng, 2010). The first ten volumes of each subject were removed for signal equilibrium and to allow the participants' adaptation to the scanning noise. After slice timing and movement correction, all the rs-fMRI images were normalized to the Montreal Neurological Institute EPI template with voxel size 3×3×3 mm^3 and smoothed with a 6 mm full-width at half-maximum isotropic Gaussian kernel to increase the signal-to-noise ratio. Linear drift correction was applied, and a band-pass filter with cut-off frequencies of 0.01 and 0.10 Hz was used to eliminate the effects of both very low and high frequency physiological noise (respiratory and cardiac signals). Nuisance covariates were regressed out: the whole-brain signal was removed to reduce the effect of physiological artifacts, since the global signal has been found to be associated with respiration-induced fMRI signal (Birn *et al.*, 2006); six motion parameters, the cerebrospinal fluid and the white matter signals were removed to reduce the effects of head motion and non-neuronal blood oxygenation level-dependent (BOLD) signal fluctuations.

Then, the cross-correlations of spontaneous BOLD signal fluctuations, which may reflect the inter-regional correlations in neuronal variability, were computed to assess the signal synchrony among remote brain areas. Specifically, we were interested in investigating the rsFC of the M1, which is involved in both the neural circuits influencing the velocity and transition kinematic processes in motor sequence learning (Orban *et al.*, 2011). Since the

subjects were asked to perform the finger motor sequence with the right hand, we estimated the rsFC of the left M1 with all the other voxels in the brain.

To this aim, a Region of Interest (ROI) including the left M1 was selected from the Anatomical Automatic Labeling template (Tzourio-Mazoyer *et al.*, 2002) and defined as the seed region for each participant. Analogously, we also considered the right M1, and the left and right SMA. The averaged time course was obtained from **each ROI** and the correlation analysis was performed in a voxel-wise way to generate the rsFC map of **each ROI**, called the "**ROI-**rsFC map". Finally, the obtained correlation coefficient maps were converted into z maps by Fisher's r-to-z transform to improve the normality generating a "**ROI-**zrsFC map" **for each ROI** for each subject.

Motor sequence learning analysis

Motor behavioral data were acquired by the glove system at 1 kHz and processed with customized software to extract the following parameters: Touch Duration (TD), i.e., the contact time between the thumb and another finger (ms), and Inter Tapping Interval (ITI), i.e., the time interval between the end of a thumb-to-finger contact and the beginning of the subsequent contact in the finger motor sequence (ms). Hence, movement rate (RATE), representing the number of finger taps per second (Hz), was derived for each finger opposition movement as the inverse of the interval between the beginning of a touch and the beginning of the successive one.

These parameters were averaged on each trial, thus for each subject we obtained fifty values of each parameter over the time course of the learning task. The ability to learn the finger motor sequence was assessed by changes in RATE, while the strategy adopted by each subject to accomplish this goal was evaluated by the analysis of changes in TD and ITI (Bove *et al.*, 2007). In details, the first trial was used to familiarize the subjects with the task and the glove system; the average of each parameter between the values obtained in the second and third trials was considered as the initial performance (baselineRATE (Hz), baselineTD (ms) and baselineITI (ms)), while the average between the forty-ninth and the fiftieth trials indicated the level of performance achieved at the end of the task. Considering that an increase in RATE and a decrease in TD and ITI were indicators of performance improvement, changes in the different parameters were calculated as follows: the final value minus the initial value for RATE, the initial value minus the final value for TD and ITI. The resulting parameters were referred to as: deltaRATE (Hz), deltaTD (ms) and deltaITI (ms). Curve fitting was also performed to indicate the mean group learning curve for the different kinematic parameters.

Statistics

From the analysis of rs-fMRI, in order to explore the within-group pattern of rsFC with the **selected motor areas**, one-sample t-test was performed **separately** on the leftM1-zrsFC, **rightM1-zrsFC, leftSMA-zrsFC and rightSMA-zrsFC** maps by using SPM8 (http://www.fil.ion.ucl.ac.uk/spm/). A height threshold of $p<0.001$ uncorrected was applied; the minimum cluster size was arbitrarily set to 10 voxels.

For each ROI, we then implemented three second-level analyses with a regression model based on the single-subject zrsFC maps, considering the deltaRATE, deltaTD and deltaITI values of each subject as covariates. We thus obtained a group map for each different seed indicating the significant correlation between the z-values of connectivity and each of the parameters related to motor sequence learning, with a height threshold of $p<0.001$ uncorrected and minimum cluster size of 10 voxels. For left M1, which constituted the specific target of this work, similar regression analyses were performed with RATE, TD, and ITI values at baseline as covariates (i.e., baselineRATE, baselineTD, baselineITI).

The Talairach Daemon server data (http://www.talairach.org/daemon.html) was searched using x,y,z coordinates after conversion from MNI to Talairach space to localize significant clusters. Xjview (http://www.alivelearn.net/xjview8/) was then used to display images in MNI space and improve anatomy description, especially to define cerebellar regions and thalamus subdivisions.

To evaluate the dynamics of motor performance over the time course of the learning task, RATE, TD and ITI were entered separately for each subject in a one-way repeated-measures analysis of variance (RM-ANOVA), with time (trial number) as main factor. Significant main effects were explored with the Newman-Keuls post-hoc test.

Results

Motor sequence learning

All subjects well tolerated the entire experimental protocol and were able to learn the proposed sequence by verbal code and to reproduce it with the finger touches, as requested, without errors. They all improved their performance with practice, in fact they showed a significant increase in their RATE values, obtained by significantly reducing both TD and ITI values (RM-ANOVA: RATE: $F(49,637)=50.71$, $p<0.0001$; TD: $F(49,637)=19.61$, $p<0.0001$; ITI: $F(49,637)=16.71$, $p<0.0001$). The three motor parameters are reported as a function of time, i.e., trial number (RATE is shown in Figure 2A; TD and ITI in Figure 2B and C, respectively).

Specifically, on average TD significantly decreased from trial 3 ($p=0.02$ with respect to trial 1) and reached a value similar to the final value from trial 14 ($p=0.08$ with respect to trial 50); ITI significantly decreased from trial 3 ($p=0.004$ with respect to trial 1) and reached a value similar to the final value from trial 13 ($p=0.24$ with respect to trial 50). As a consequence, RATE significantly increased from trial 3 ($p=0.01$ with respect to trial 1) and reached a value similar to the final value from trial 29 ($p=0.26$ with respect to trial 50). Thus, at the end of the learning task the single subjects had a performance gain in motor sequence learning skills given by deltaRATE, deltaTD and deltaITI. All measures were normally distributed, as determined by the Shapiro-Wilk test. The kinematic data were fitted to indicate the mean group learning curve: the best model was Gaussian for RATE ($y = y_0 + (A/(w\times\sqrt{(\pi/2)}))\times\exp(-2\times((x-x_c)/w)^2)$, $x_c = 45.79 \pm 3.841$, $w = 119.53 \pm 99.83$, $R^2 = 0.99$), exponential for TD ($y = A_1\times\exp(-x/t_1) + y0$, $t_1 = 11.83 \pm 1.15$, $R^2 = 0.98$) and ITI ($y = A_1\times\exp(-x/t_1) + y0$, $t_1 = 12.14 \pm 1.34$, $R^2 = 0.94$).

Resting-state fMRI

Left M1—From the analysis of the rsFC of the left M1, we obtained a leftM1-zrsFC map of the group of subjects, showing that at rest the left M1 was strongly functionally connected with other motor areas, such as the left premotor cortex (PMC) and SMA, corresponding to the Brodmann area (BA) 6, and also with other areas belonging to the temporal, cingulate and occipital (visual) cortex (Figure 3**A** and Table 1).

Further, the regression model implemented on the leftM1-zrsFC group map with deltaRATE as covariate showed only one significant cluster in the right cerebellum (Figure 4A and Table 2), indicating that the subjects who were able to increase more their RATE with practice were those showing stronger rsFC between the left M1 and the right cerebellar hemisphere at rest, and in particular with the lobule VIII.

Looking at the different possible strategies to adopt in order to increase RATE (i.e., reducing TD, ITI, or both), when deltaTD was considered as covariate we found significant clusters located in the left cerebellum and in the right and left association nuclei of the thalamus (Figure **4B and Table 2**). In details, the lobule VIIb, the Crus I, and the lobule IV-V of the cerebellum, and the Pulvinar and the dorsomedial nucleus of the thalamus were identified. Taking into account deltaITI as covariate, we found that the subjects who reduced more their ITI values were those showing stronger rsFC of the left M1 with the right association nuclei of the thalamus (Pulvinar, dorsomedial nucleus and anterior nucleus) and the left cerebellum (lobule IV-V and lobule VI) (Figure **4C and Table 2**). Further, we also assessed the correlation between the rsFC of the left M1 and the initial motor performance of the subjects; the regression models implemented on the leftM1-zrsFC group map with baselineTD and baselineITI showed clusters similar to those obtained by the regression models with gain in these kinematic parameters during the motor learning (i.e., deltaTD and deltaITI). In particular, we observed that lower values of baselineTD correlated with stronger rsFC of the left M1 with the lobule VIIb and the lobule IV-V of the left cerebellum and the Pulvinar while lower values of baselineITI correlated with stronger rsFC of the left M1 with the right association nuclei of the thalamus (Pulvinar, dorsomedial nucleus and anterior nucleus) and the left cerebellum (lobule IV-V and lobule VI) (Table 3). On the other hand, higher values of baselineRATE did not refer with the clusters observed in the correlation analysis between rsFC left M1 and deltaRATE but with sensory areas such as BA1 and BA3 (Table 3).

Right M1—Similarly to the left M1 seed, from the analysis of the rsFC of the right M1, we obtained a rightM1-zrsFC map of the group of subjects, showing that at rest the right M1 was strongly functionally connected with other motor areas, such as the PMC and SMA, corresponding to the Brodmann area (BA) 6, and also with other areas belonging to the temporal, cingulate and occipital (visual) cortex (Figure 3B and Table 4).

However, differently from the results obtained from the left M1 seed analysis the regression model implemented on the rightM1-zrsFC group map with deltaRATE or deltaITI as covariate showed no significant cluster and only one significant cluster related to the right frontal lobe was observed when deltaTD was used as covariate in the analysis (Figure 4D and Table 5).

Left SMA—From the analysis of the rsFC of the left SMA, we obtained a leftSMA-zrsFC map of the group of subjects, showing that at rest the left SMA was strongly functionally connected with other motor areas, such as the left and right PMC and SMA, corresponding to the Brodmann area (BA) 6, and also with other areas belonging to the prefrontal, temporal and insular cortex (Figure 3C and Table 6).

The regression model implemented on the leftSMA-zrsFC group map with deltaRATE as covariate showed two significant clusters: one in the right cerebellum, and in particular in the lobule VIII as observed in the left M1 seed analysis with deltaRATE as covariate and another cluster in the right orbitofrontal cortex (Figure 5A and Table 7). When deltaTD was considered as covariate we found a significant cluster located in the left cingulate cortex (Figure 5B and Table 7). Taking into account deltaITI as covariate, we found that the subjects who reduced more their ITI values were those showing stronger rsFC of the left SMA with the association nuclei of the thalamus (Pulvinar, and anterior nucleus) and the cingulate cortex (Figure 5C and Table 7).

Right SMA—Similarly to the analysis of the rsFC of the left SMA, for the right SMA we obtained a rightSMA-zrsFC map of the group of subjects, showing that at rest the right SMA was strongly functionally connected with other motor areas, such as the right PMC and SMA (BA 6), and also with other areas belonging to the prefrontal, temporal and insular cortex (Figure 3D and Table 8).

Only the regression model implemented on the leftSMA-zrsFC group map with deltaRATE as covariate showed significant clusters, whilst no significant cluster was observed with deltaTD or deltaITI as covariate. In detail, with deltaRATE as covariate we found that the subjects who increased more their RATE values were those showing stronger rsFC of the right SMA with the right orbitofrontal and temporal cortex (Figure 5D and Table 9).

Discussion

In this work, we showed that the repetition of an already verbally-learned sequence of finger opposition movements leads to an improvement in motor performance characterized by an increase in movement execution rate. This is in line with several works showing that the repetition of a motor sequence progressively reduces the time of its execution (Korman *et al.*, 2003; Orban *et al.*, 2011; Walker *et al.*, 2003). We also showed that the improvement in motor sequence performance can be achieved through the reduction of touch duration (TD) or inter tapping interval (ITI) or both, parameters describing specific aspects of the performance of a sequence of finger opposition movements. From a functional point of view, TD, i.e., the time spent in the contact between the thumb and another finger of the sequence, involves both a pure “sensory time” needed for an adequate perception of the touched finger before moving forwards in the finger motor opposition movements sequence, and a “preparatory time” needed to plan the next correct movement in the sequence, whilst ITI, i.e., the time interval between two successive thumb contacts in the finger motor sequence, can be interpreted as a pure “motor time” (Avanzino *et al.*, 2008). Therefore, at the end of the learning task each subject showed a performance gain in motor sequence

learning characterized by an increase in movement rate (deltaRATE), achieved by means of reductions of in TD and/or ITI values (deltaTD and deltaITI).

Since short-term motor practice or learning of novel motor sequences results in plasticity of the **motor areas** (Classen *et al.*, 1998; Lotze *et al.*, 2003; Morgen *et al.*, 2004; Muellbacher *et al.*, 2001; Muellbacher *et al.*, 2002; Orban *et al.*, 2011) we identified the left and right M1 and the left and right SMA as the seeds of our rsFC analysis and we cross-correlated the time course of **each** seed with that of all other voxels in the brain. We thus obtained a group rsFC for each seed, showing that at rest both M1 and SMAs were mainly connected with other brain motor areas, such as the premotor cortex and the supplementary motor area (Langan *et al.*, 2010; Xiong *et al.*, 1999), whilst no evidence of significant functional connectivity of these areas with subcortical circuits, such as the basal ganglia or the cerebellum, was found. This is not surprising since the functional connectivity between subcortical structures and the cortex is usually investigated with different methodological approaches (Bernard *et al.*, 2012; Buckner *et al.*, 2011; O'Reilly *et al.*, 2010). When we added to our seed-based whole-brain analysis the three investigated kinematic parameters indicating motor learning improvement as covariates, the neural structures showing significant rsFC with the left M1 were found to be the cerebellum and the thalamus. Similar results were obtained for the left SMA, also including the orbital and cingulate cortex. Indeed, the subjects who achieved greater RATE increase with practice were those showing stronger rsFC of the left M1 and of the left SMA with the right lobule VIII of the cerebellum. Furthermore, when deltaITI was considered as covariate, the subjects with greater ITI reduction showed stronger rsFC of the left M1 and the left SMA with the association nuclei of the thalamus (Pulvinar and anterior nucleus). Conversely, the same regression analysis with the right M1 and SMA seeds showed only few significant clusters for the different covariates not located in the cerebellum and thalamus. No common clusters were found between right M1 and SMA. All these findings could indicate high specificity of the resting neural circuits responsible of motor performance improvement during motor learning involving the motor areas related to the hemisphere directly controlling the finger movements, the thalamus and the cerebellum.

In particular, different parts of the cerebellum were strongly correlated with the rsFC of the left M1 for the different covariates. Indeed, when deltaTD was considered as covariate we found significant clusters located in the left cerebellum, such as the lobule VIIb, the Crus I, and the lobule IV-V,whereas when deltaITI was considered as covariate with the left cerebellum (lobule IV-V and lobule VI). Our findings are in line with a recent study demonstrating the involvement of the cerebellar lobules IV–VI and VIII in the sensorimotor network (Sang *et al.*, 2012). Indeed, rsFC studies point to the existence of segregated functional cerebello-cerebral networks in humans, including a sensorimotor network encompassing the cerebellar lobules VIII and IV-VI and the primary motor cortex (Krienen & Buckner, 2009; O'Reilly *et al.*, 2010). In addition, transneuronal tracers in monkeys showed the existence of anatomical projections between the arm areas of both cerebral and cerebellar motor regions (Kelly & Strick, 2003). Neuroimaging studies have also revealed that the anterior lobe (lobules I–V) and part of the posterior lobe (lobules VI and VIII) of the cerebellum are sensorimotor components (Stoodley & Schmahmann, 2010). Finally, a meta-

analysis of functional topography in the human cerebellum showed consistent activation in lobules V, VI and VIII during motor and somatosensory tasks (Stoodley & Schmahmann, 2009). Interestingly, lobules IV-V are common for deltaTD and deltaITI covariate analyses underlying the importance of a priori functional connection between the left M1 and these regions to allow a significant gain in the different components of a sequence learning task. Accordingly, a recent fMRI study showed that the velocity and the transition variables measured during finger motor sequence learning strongly correlated with the activation of the same cerebellar regions found in our work (Orban *et al.*, 2011). Similarly, cerebellar lobules IV–V were common for the two variables whilst lobule VIII only correlated with the velocity. Although in our work finger movement rate was measured differently from Orban *et al.* (2011), we noted the importance of higher functional connectivity between the left M1 and this region in allowing a significant increase in the execution rate of the motor sequence.

In addition to cerebellar regions involved in the sensorimotor network, significant clusters were observed in the left cerebellum, in the lobule VIIb and Crus I, when deltaTD was considered as covariate. In a recent work, lobule VIIb and Crus I have been found to correlate with the SMA and parts of the lateral motor cortex, supporting the idea that lobule VII is involved in complex movements (Schlerf *et al.*, 2010). Further, other works showed the importance of these motor-related cerebellar subregions in processing various dexterous motions, such as hand movement (Chan *et al.*, 2006; Nitschke *et al.*, 2005) and finger tapping (Aoki *et al.*, 2005; Witt *et al.*, 2008). Finally, anatomical studies in monkeys showed interconnections between the prefrontal cortex and lobule VII (Crus I, Crus II, and lobule VIIB) (Kelly & Strick, 2003).

Taken together these findings suggest that, although TD and ITI share the same sensorimotor network for the accomplishment of the motor sequence learning task, regions of the cerebellum belonging to the fronto-parietal network have to be active concomitantly with the primary motor area at rest to obtain an increase in performance rate through a reduction of TD. Indeed, to significantly reduce TD it is necessary to have an adequate perception of the touched finger before moving forwards in the finger motor sequence (i.e., spatial function), and concomitantly to plan the next correct movement in the sequence (i.e., executive function).

Contralateral mapping between cortical masks and strength of correlation in the cerebellum is usually found (O'Reilly *et al.*, 2010). Therefore, the difference in rsFC lateralization between leftM1 and the cerebellum found with deltaRATE (i.e., contralateral) and with deltaTD or deltaITI (i.e., ipsilateral) could be unexpected. However, we cannot exclude that M1 functional connectivity can be higher with the ipsilateral cerebellum than with the contralateral one when rsFC analysis is associated with a parameter describing the attitude to achieve a specific function in a task. Indeed, clinical and imaging studies have indicated that language representation in the cerebellum is more right-lateralized, while spatial functions are more left-lateralized (see for a review (Stoodley & Schmahmann, 2009). These results are in agreement with findings in non-human primates suggesting that not all cerebro-pontocerebellar projections are crossed (Brodal, 1979).

The regression analysis **with left M1 and left SMA as seeds** also identified the association nuclei of the thalamus (Pulvinar, dorsomedial nucleus and anterior nucleus) as neural structures playing a key role to significantly reduce TD and ITI improving motor performance (**RATE**). Among the different functions of these nuclei concerning motor behavior, it has been suggested that they may play a role in emotional learning (Oyoshi *et al.*, 1996). Notably, we found that subjects showing greater improvement in RATE with practice were those showing significant rsFC of the two SMAs with the right orbitofrontal cortex. Therefore, we can speculate that higher gains in a motor sequence learning task might occur in those subjects who have an important functional connection at rest between the motor areas and the neural structures mediating information from the limbic part of the brain. New evidence confirms that interactions among cortico– cerebellar and limbic structures are crucial for building the motor memory trace (Doyon & Benali, 2005).

Although the association nuclei of the thalamus are anatomically and functionally connected with the basal ganglia we did not find any co-activation with these subcortical structures in the covariate analysis. One possible explanation could be that the functional interactions of these regions are more variable, accommodating specific task demands by flexibly interacting with demand-specific regions for short periods of time (Deco *et al.*, 2011; Mennes *et al.*, 2013). This hypothesis is consistent with models of basal ganglia and thalamic anatomical connectivity emphasizing parallel but integrated cognitive, emotional, and motor circuits supporting flexible adaptation to internal and external demands (Alexander *et al.*, 1990; Bonzano *et al.*, 2013; Haber, 2003). Numerous studies have demonstrated that the cerebellum is active during the fast learning phase, but that this activity decreases with practice and may become undetectable when the sequential movements are well learned (see for a review (Doyon *et al.*, 2003)).

Finally, when assessing the correlation between the rsFC of left M1 and the initial motor performance of the subjects we found that lower values of TD correlated with stronger rsFC of the left M1 with the lobule VIIb and the lobule IV-V of the left cerebellum and the Pulvinar while lower values of ITI correlated with stronger rsFC of the left M1 with the right association nuclei of the thalamus (Pulvinar, dorsomedial nucleus and anterior nucleus) and the left cerebellum (lobule IV-V and lobule VI). These are the same clusters obtained by the regression models with the gain in these kinematic parameters at the end of the motor learning task. These findings might indicate that the rsFC among these neural structures is not only important to give an indication of the final motor performance gain but it can be also an index of the motor strategy adopted by the subjects at baseline.

To conclude, our results show that the brain functional architecture at rest does not provide a complete representation of its repertoire of extrinsic responses that can be found for instance in the case of motor sequence learning. It has been demonstrated that intrinsic approaches provide only partial understanding of brain functional architecture confirming that task-based fMRI approaches are required to appreciate the full repertoire of dynamic neural responses (Mennes *et al.*, 2013). Here we propose a complementary method in which the correlation between brain rsFC and sensorimotor behavioral measurements might reveal some different regions necessary to successfully achieve a specific motor task. We think that

this approach could help understand impairments in sensorimotor task performance in neurological disorders, and aid in the design of appropriate rehabilitative treatments.

Acknowledgments

This study was supported in part by the National Institutes of Health grant number R56NS051623 and by the Noto Foundation to MI.

Abbreviations

BA	Brodmann area
fMRI	functional magnetic resonance imaging
ITI	Inter Tapping Interval
M1	primary motor cortex
PMC	premotor cortex
RM-ANOVA	repeated-measures analysis of variance
rs-fMRI	resting-state fMRI
rsFC	resting-state functional connectivity
SMA	supplementary motor area
TD	Touch Duration

References

Aertsen AM, Gerstein GL, Habib MK, Palm G. Dynamics of neuronal firing correlation: modulation of “effective connectivity”. J Neurophysiol. 1989; 61:900–917. [PubMed: 2723733]

Albert NB, Robertson EM, Miall RC. The resting human brain and motor learning. Curr Biol. 2009; 19:1023–1027. [PubMed: 19427210]

Alexander GE, Crutcher MD, DeLong MR. Basal ganglia-thalamocortical circuits: parallel substrates for motor, oculomotor, “prefrontal” and “limbic” functions. Prog Brain Res. 1990; 85:119–146. [PubMed: 2094891]

Aoki T, Tsuda H, Takasawa M, Osaki Y, Oku N, Hatazawa J, Kinoshita H. The effect of tapping finger and mode differences on cortical and subcortical activities: a PET study. Exp Brain Res. 2005; 160:375–383. [PubMed: 15368088]

Ashe J, Lungu OV, Basford AT, Lu X. Cortical control of motor sequences. Curr Opin Neurobiol. 2006; 16:213–221. [PubMed: 16563734]

Avanzino L, Bove M, Trompetto C, Tacchino A, Ogliastro C, Abbruzzese G. 1-Hz repetitive TMS over ipsilateral motor cortex influences the performance of sequential finger movements of different complexity. Eur J Neurosci. 2008; 27:1285–1291. [PubMed: 18312586]

Bernard JA, Seidler RD, Hassevoort KM, Benson BL, Welsh RC, Wiggins JL, Jaeggi SM, Buschkuehl M, Monk CS, Jonides J, Peltier SJ. Resting state cortico-cerebellar functional connectivity networks: a comparison of anatomical and self-organizing map approaches. Front Neuroanat. 2012; 6:31. [PubMed: 22907994]

Birn RM, Diamond JB, Smith MA, Bandettini PA. Separating respiratory-variation-related fluctuations from neuronal-activity-related fluctuations in fMRI. Neuroimage. 2006; 31:1536–1548. [PubMed: 16632379]

Biswal B, Yetkin FZ, Haughton VM, Hyde JS. Functional connectivity in the motor cortex of resting human brain using echo-planar MRI. Magn Reson Med. 1995; 34:537–541. [PubMed: 8524021]

Bonzano L, Tacchino A, Saitta L, Roccatagliata L, Avanzino L, Mancardi GL, Bove M. Basal ganglia are active during motor performance recovery after a demanding motor task. Neuroimage. 2013; 65:257–266. [PubMed: 23063450]

Bove M, Tacchino A, Novellino A, Trompetto C, Abbruzzese G, Ghilardi MF. The effects of rate and sequence complexity on repetitive finger movements. Brain Res. 2007; 1153:84–91. [PubMed: 17459347]

Buckner RL, Krienen FM, Castellanos A, Diaz JC, Yeo BT. The organization of the human cerebellum estimated by intrinsic functional connectivity. J Neurophysiol. 2011; 106:2322–2345. [PubMed: 21795627]

Chan RC, Rao H, Chen EE, Ye B, Zhang C. The neural basis of motor sequencing: an fMRI study of healthy subjects. Neurosci Lett. 2006; 398:189–194. [PubMed: 16469446]

Chao-Gan Y, Yu-Feng Z. DPARSF: A MATLAB Toolbox for "Pipeline" Data Analysis of Resting-State fMRI. Front Syst Neurosci. 2010; 4:13. [PubMed: 20577591]

Classen J, Liepert J, Wise SP, Hallett M, Cohen LG. Rapid plasticity of human cortical movement representation induced by practice. J Neurophysiol. 1998; 79:1117–1123. [PubMed: 9463469]

Deco G, Jirsa VK, McIntosh AR. Emerging concepts for the dynamical organization of resting-state activity in the brain. Nat Rev Neurosci. 2011; 12:43–56. [PubMed: 21170073]

Doyon J, Bellec P, Amsel R, Penhune V, Monchi O, Carrier J, Lehericy S, Benali H. Contributions of the basal ganglia and functionally related brain structures to motor learning. Behav Brain Res. 2009; 199:61–75. [PubMed: 19061920]

Doyon J, Benali H. Reorganization and plasticity in the adult brain during learning of motor skills. Curr Opin Neurobiol. 2005; 15:161–167. [PubMed: 15831397]

Doyon J, Penhune V, Ungerleider LG. Distinct contribution of the cortico-striatal and cortico-cerebellar systems to motor skill learning. Neuropsychologia. 2003; 41:252–262. [PubMed: 12457751]

Friston KJ, Frith CD, Liddle PF, Frackowiak RS. Functional connectivity: the principal-component analysis of large (PET) data sets. J Cereb Blood Flow Metab. 1993; 13:5–14. [PubMed: 8417010]

Haber SN. The primate basal ganglia: parallel and integrative networks. J Chem Neuroanat. 2003; 26:317–330. [PubMed: 14729134]

Jastorff J, Kourtzi Z, Giese MA. Learning to discriminate complex movements: biological versus artificial trajectories. J Vis. 2006; 6:791–804. [PubMed: 16895459]

Kelly RM, Strick PL. Cerebellar loops with motor cortex and prefrontal cortex of a nonhuman primate. J Neurosci. 2003; 23:8432–8444. [PubMed: 12968006]

Korman M, Raz N, Flash T, Karni A. Multiple shifts in the representation of a motor sequence during the acquisition of skilled performance. Proc Natl Acad Sci U S A. 2003; 100:12492–12497. [PubMed: 14530407]

Krienen FM, Buckner RL. Segregated fronto-cerebellar circuits revealed by intrinsic functional connectivity. Cereb Cortex. 2009; 19:2485–2497. [PubMed: 19592571]

Kuriyama K, Stickgold R, Walker MP. Sleep-dependent learning and motor-skill complexity. Learn Mem. 2004; 11:705–713. [PubMed: 15576888]

Langan J, Peltier SJ, Bo J, Fling BW, Welsh RC, Seidler RD. Functional implications of age differences in motor system connectivity. Front Syst Neurosci. 2010; 4:17. [PubMed: 20589101]

Lotze M, Braun C, Birbaumer N, Anders S, Cohen LG. Motor learning elicited by voluntary drive. Brain. 2003; 126:866–872. [PubMed: 12615644]

Lowe MJ, Dzemidzic M, Lurito JT, Mathews VP, Phillips MD. Correlations in low-frequency BOLD fluctuations reflect cortico-cortical connections. Neuroimage. 2000; 12:582–587. [PubMed: 11034865]

Mennes M, Kelly C, Colcombe S, Castellanos FX, Milham MP. The extrinsic and intrinsic functional architectures of the human brain are not equivalent. Cereb Cortex. 2013; 23:223–229. [PubMed: 22298730]

Miall RC, Jackson JK. Adaptation to visual feedback delays in manual tracking: evidence against the Smith Predictor model of human visually guided action. Exp Brain Res. 2006; 172:77–84. [PubMed: 16424978]

Moisello C, Avanzino L, Tacchino A, Ruggeri P, Ghilardi MF, Bove M. Motor sequence learning: acquisition of explicit knowledge is concomitant to changes in motor strategy of finger opposition movements. Brain Res Bull. 2011; 85:104–108. [PubMed: 21459132]

Morgen K, Kadom N, Sawaki L, Tessitore A, Ohayon J, Frank J, McFarland H, Martin R, Cohen LG. Kinematic specificity of cortical reorganization associated with motor training. Neuroimage. 2004; 21:1182–1187. [PubMed: 15006685]

Muellbacher W, Ziemann U, Boroojerdi B, Cohen L, Hallett M. Role of the human motor cortex in rapid motor learning. Exp Brain Res. 2001; 136:431–438. [PubMed: 11291723]

Muellbacher W, Ziemann U, Wissel J, Dang N, Kofler M, Facchini S, Boroojerdi B, Poewe W, Hallett M. Early consolidation in human primary motor cortex. Nature. 2002; 415:640–644. [PubMed: 11807497]

Nitschke MF, Arp T, Stavrou G, Erdmann C, Heide W. The cerebellum in the cerebro-cerebellar network for the control of eye and hand movements--an fMRI study. Prog Brain Res. 2005; 148:151–164. [PubMed: 15661188]

Orban P, Peigneux P, Lungu O, Debas K, Barakat M, Bellec P, Benali H, Maquet P, Doyon J. Functional neuroanatomy associated with the expression of distinct movement kinematics in motor sequence learning. Neuroscience. 2011; 179:94–103. [PubMed: 21277942]

O'Reilly JX, Beckmann CF, Tomassini V, Ramnani N, Johansen-Berg H. Distinct and overlapping functional zones in the cerebellum defined by resting state functional connectivity. Cereb Cortex. 2010; 20:953–965. [PubMed: 19684249]

Oyoshi T, Nishijo H, Asakura T, Takamura Y, Ono T. Emotional and behavioral correlates of mediodorsal thalamic neurons during associative learning in rats. J Neurosci. 1996; 16:5812–5829. [PubMed: 8795634]

Sami S, Miall RC. Graph network analysis of immediate motor-learning induced changes in resting state BOLD. Front Hum Neurosci. 2013; 7:166. [PubMed: 23720616]

Sang L, Qin W, Liu Y, Han W, Zhang Y, Jiang T, Yu C. Resting-state functional connectivity of the vermal and hemispheric subregions of the cerebellum with both the cerebral cortical networks and subcortical structures. Neuroimage. 2012; 61:1213–1225. [PubMed: 22525876]

Schlerf JE, Verstynen TD, Ivry RB, Spencer RM. Evidence of a novel somatopic map in the human neocerebellum during complex actions. J Neurophysiol. 2010; 103:3330–3336. [PubMed: 20393055]

Sheth BR, Janvelyan D, Khan M. Practice makes imperfect: restorative effects of sleep on motor learning. PLoS One. 2008; 3:e3190. [PubMed: 18787652]

Stoodley CJ, Schmahmann JD. Functional topography in the human cerebellum: a meta-analysis of neuroimaging studies. Neuroimage. 2009; 44:489–501. [PubMed: 18835452]

Stoodley CJ, Schmahmann JD. Evidence for topographic organization in the cerebellum of motor control versus cognitive and affective processing. Cortex. 2010; 46:831–844. [PubMed: 20152963]

Tzourio-Mazoyer N, Landeau B, Papathanassiou D, Crivello F, Etard O, Delcroix N, Mazoyer B, Joliot M. Automated anatomical labeling of activations in SPM using a macroscopic anatomical parcellation of the MNI MRI single-subject brain. Neuroimage. 2002; 15:273–289. [PubMed: 11771995]

Vahdat S, Darainy M, Milner TE, Ostry DJ. Functionally specific changes in resting-state sensorimotor networks after motor learning. J Neurosci. 2011; 31:16907–16915. [PubMed: 22114261]

Walker MP, Brakefield T, Hobson JA, Stickgold R. Dissociable stages of human memory consolidation and reconsolidation. Nature. 2003; 425:616–620. [PubMed: 14534587]

Witt ST, Laird AR, Meyerand ME. Functional neuroimaging correlates of finger-tapping task variations: an ALE meta-analysis. Neuroimage. 2008; 42:343–356. [PubMed: 18511305]

Xiong J, Parsons LM, Gao JH, Fox PT. Interregional connectivity to primary motor cortex revealed using MRI resting state images. Hum Brain Mapp. 1999; 8:151–156. [PubMed: 10524607]

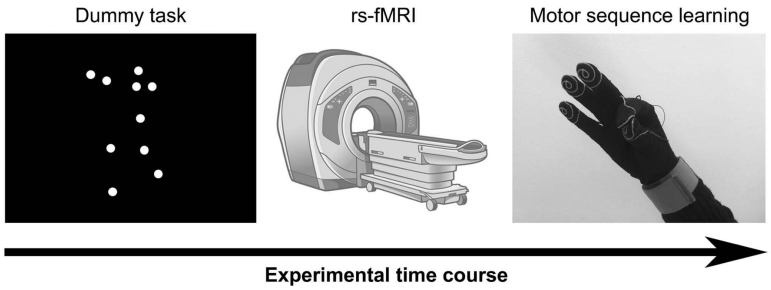

Figure 1.

Experimental protocol. Participants were shown a dummy task on the computer screen immediately before the rs-fMRI session, then they had to perform the motor sequence learning task.

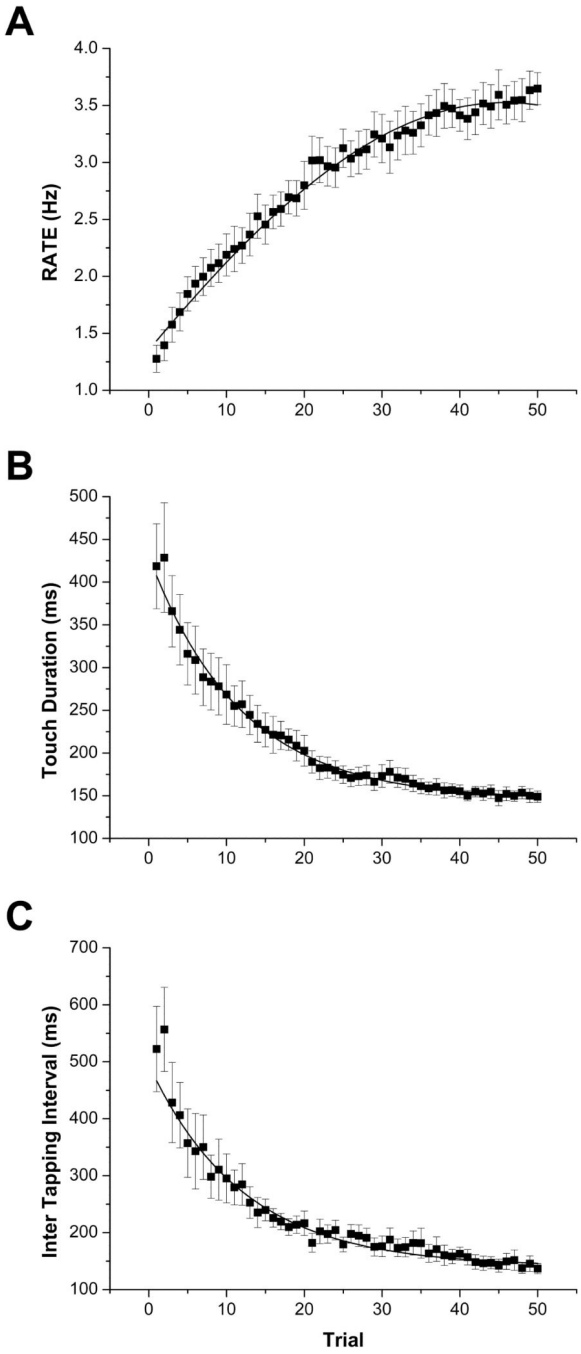

Figure 2.

Group-averaged motor parameters over the course of the motor sequence learning task (mean ± SE): **A** RATE, **B** Touch Duration (TD), **C** Inter Tapping Interval (ITI). The solid lines indicate the best fits to the data, representing the mean group learning curve: A Gaussian ($y = y_0 + (A/(w\times\sqrt{(\pi/2)}))\times\exp(-2\times((x-x_c)/w)^2)$, $x_c = 45.79 \pm 3.841$, $w = 119.53 \pm 99.83$, $R^2 = 0.99$), B Exponential ($y = A_1\times\exp(-x/t_1) + y0$, $t_1 = 11.83 \pm 1.15$, $R^2 = 0.98$), C Exponential ($y = A_1\times\exp(-x/t_1) + y0$, $t_1 = 12.14 \pm 1.34$, $R^2 = 0.94$).

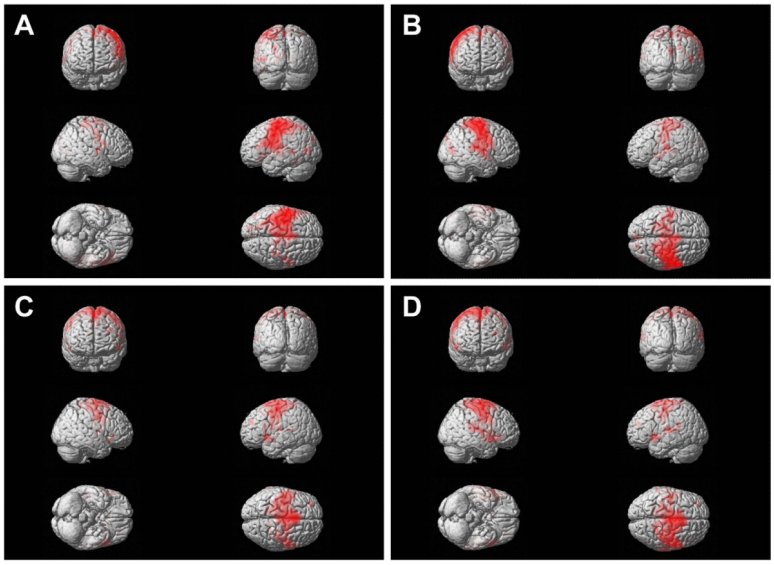

Figure 3.

Whole-brain seed-based resting functional connectivity maps of the selected seeds in the motor areas, displayed on a volumetric brain surface: A left M1, B right M1, C left SMA, D right SMA. Significant clusters are displayed in neurological convention (the left side of the image corresponds to the left side of the brain). See Tables 1, 4, 6, and 8.

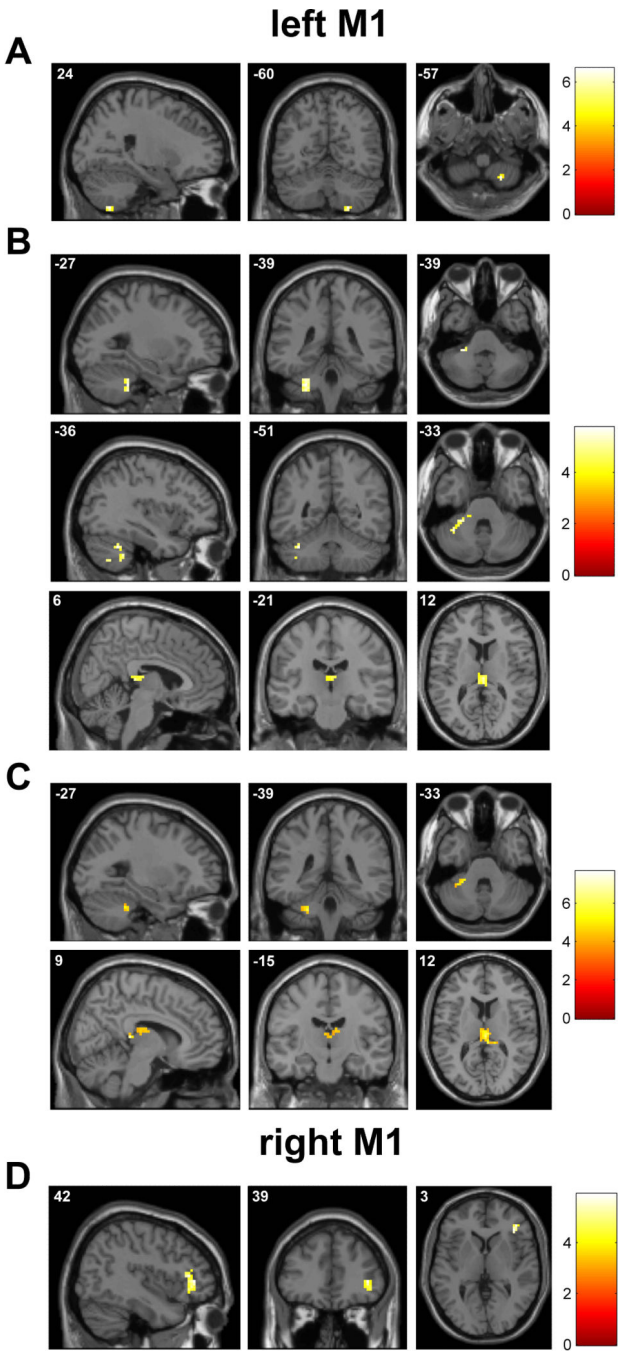

Figure 4.

Regression analysis between the resting functional connectivity maps of the M1 areas and the kinematic parameters indicating motor learning improvement: A left M1 with deltaRATE as covariate, B left M1 with deltaTD, C left M1 with deltaITI, D right M1 with deltaTD. Significant clusters are displayed in neurological convention; color bar shows a scale of T values. See Tables 2 and 5.

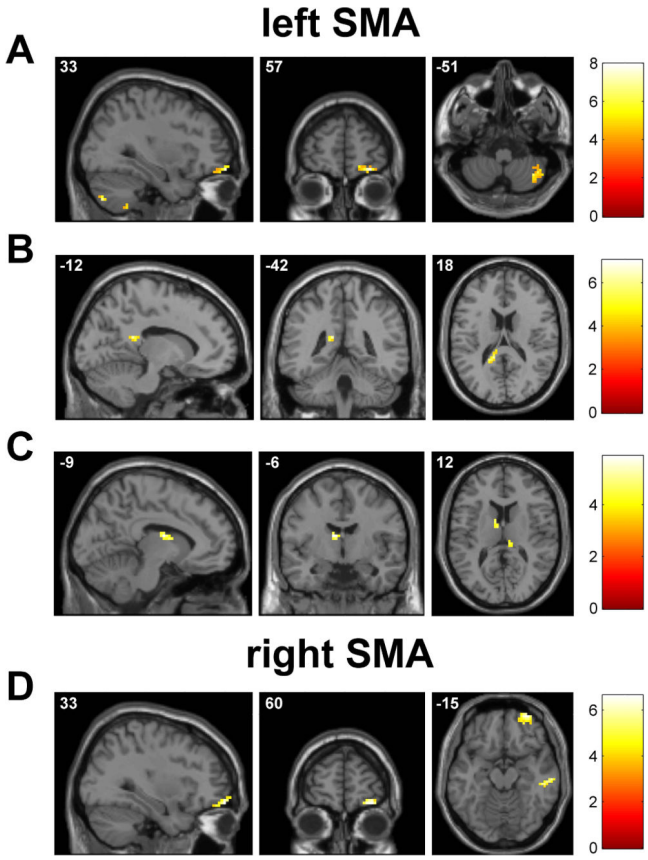

Figure 5.

Regression analysis between the resting functional connectivity maps of the SMAs and the kinematic parameters indicating motor learning improvement: A left SMA with deltaRATE as covariate, B left SMA with deltaTD, C left SMA with deltaITI, D right SMA with deltaRATE. Significant clusters are displayed in neurological convention; color bar shows a scale of T values. See Tables 7 and 9.

Table 1

Brain regions showing significant functional connectivity with the left M1 at rest.

Cluster Size	Voxel T	Voxel Z	MNI Coordinate: x y z (mm)	Region (Brodmann area)
5117	16.45	6.24	−57 0 39	6
	16.22	6.21	−42 0 57	6
	15.80	6.16	−39 −15 66	6
236	8.47	4.86	−15 −75 9	17
	5.78	4.00	−21 −63 6	30
	5.26	3.79	−15 −84 9	17
78	7.77	4.67	−54 −42 3	22
	5.50	3.89	−63 −39 6	22
	4.68	3.52	−54 −42 12	22
58	6.84	4.38	−42 −78 6	19
	5.77	3.99	−54 −69 6	37
50	6.26	4.18	15 −66 9	30
	5.17	3.75	15 −75 6	23
	4.62	3.49	21 −69 0	19
36	4.81	3.58	−51 −51 −18	20
	4.79	3.57	−45 −39 −21	37
	4.10	3.23	−48 −54 −6	37
21	5.79	4.00	27 −3 45	6
	4.61	3.49	36 −3 48	6

Height threshold: T = 3.85 (uncorrected $p<0.001$); extent threshold: k = 10 voxels.

Table 2

Significant results from the regression analysis performed on the map of functional connectivity with the left M1 at rest, considering deltaRATE, deltaTD and deltaITI as covariate.

Kinematic covariate	Cluster Size	Voxel T	Voxel Z	MNI Coordinate: x y z (mm)	Region
deltaRATE	10	6.61	4.21	24 −60 −57	Cerebellum (lobule VIII)
deltaTD	68	5.74	3.91	−27 −39 −39	Cerebellum (lobule VIIb)
		5.59	3.85	−36 −51 −33	Cerebellum (Crus I)
		5.27	3.72	−18 −30 −21	Cerebellum (lobule IV-V)
	44	5.21	3.70	6 −21 12	Thalamus (dorsomedial nucleus)
		4.49	3.38	−3 −30 12	Thalamus (Pulvinar)
		4.49	3.37	−3 −21 12	Thalamus (dorsomedial nucleus)
deltaITI	86	7.66	4.53	12 −33 9	Thalamus (Pulvinar)
		6.63	4.22	6 −21 12	Thalamus (dorsomedial nucleus)
		4.47	3.37	9 −15 18	Thalamus (anterior nucleus)
	15	5.89	3.96	−24 −36 −36	Cerebellum (lobule IV-V)
		5.25	3.71	−33 −45 −33	Cerebellum (lobule VI)

Height threshold: T = 3.93 (uncorrected p<0.001); extent threshold: k = 10 voxels.

Table 3

Significant results from the regression analysis performed on the map of functional connectivity with the left M1 at rest, considering baselineRATE, baselineTD and baselineITI as covariate.

Kinematic covariate	Cluster Size	Voxel T	Voxel Z	MNI Coordinate: x y z (mm)	Region
baselineRATE	25	5.37	3.76	66 −12 24	BA 3
		4.93	3.58	69 −15 30	BA 1
baselineTD	47	6.08	4.03	−18 −30 −21	Cerebellum (lobule IV-V)
		6.06	4.02	−27 −39 −39	Cerebellum (lobule VIIb)
		5.07	3.64	−21 −36 −30	Cerebellum (lobule IV-V)
	22	5.00	3.61	6 −30 9	Thalamus (Pulvinar)
baselineITI	111	7.53	4.50	3 −18 12	Thalamus (dorsomedial nucleus)
		6.71	4.25	12 −33 9	Thalamus (Pulvinar)
		4.87	3.55	9 −15 18	Thalamus (anterior nucleus)
	42	5.94	3.98	−27 −39 −36	Cerebellum (lobule VI)
		5.80	3.93	−18 −33 −27	Cerebellum (lobule IV-V)

BA = Brodman in area

Height threshold: T = 3.93 (uncorrected $p<0.001$); extent threshold: k = 10 voxels.

Table 4

Brain regions showing significant functional connectivity with the right M1 at rest.

Cluster Size	Voxel T	Voxel Z	MNI Coordinate: x y z (mm)	Region (Brodmann area)
5766	20.18	6.63	27 −15 72	6
	16.21	6.21	54 −9 54	6
	15.52	6.13	39 −24 69	6
47	6.64	4.31	18 −69 3	30
	4.89	3.62	24 −66 15	31
	4.58	3.47	18 −81 9	17
86	6.57	4.29	42 −75 9	39
50	5.96	4.07	24 −54 −3	19
95	5.11	3.72	0 −87 30	19
	4.96	3.65	3 −78 21	18
	4.3	3.33	−3 −90 18	18
63	5.07	3.7	18 −87 39	19
	5.06	3.7	24 −81 27	31
	4.71	3.54	30 −81 21	19

Height threshold: T = 3.85 (uncorrected $p<0.001$); extent threshold: k = 10 voxels.

Table 5

Significant results from the regression analysis performed on the map of functional connectivity with the right M1 at rest, considering deltaRATE, deltaTD and deltaITI as covariate.

Kinematic covariate	Cluster Size	Voxel T	Voxel Z	MNI Coordinate: x y z (mm)	Region (Brodmann area)
deltaRATE				No suprathreshold clusters	
deltaTD	53	5.9	3.97	42 39 3	46
		5.38	3.77	39 33 −6	47
deltaITI				No suprathreshold clusters	

Height threshold: T = 3.93 (uncorrected p<0.001); extent threshold: k = 10 voxels.

Table 6

Brain regions showing significant functional connectivity with the left SMA at rest.

Cluster Size	Voxel T	Voxel Z	MNI Coordinate: x y z (mm)	Region (Brodmann area)
4601	28.52	7.25	−3 9 60	6
	16.36	6.23	−30 −6 60	6
	13.87	5.9	−3 −6 63	6
231	10.47	5.32	−54 12 −6	22
	7.12	4.47	−54 18 18	45
	6.48	4.26	−57 0 −9	21
62	8.6	4.89	−27 48 27	10
	6.72	4.34	−33 45 33	9
47	7.58	4.61	51 21 −15	38
	6	4.08	51 30 −6	47
	5.48	3.88	57 15 −12	38
25	6.19	4.15	48 −27 −12	22
	4.54	3.45	48 −18 −24	20
34	5.26	3.78	60 0 12	6
	4.52	3.44	66 −6 3	22
	3.92	3.13	69 −12 15	43
35	4.68	3.52	−66 −48 15	22
	4.62	3.49	−57 −39 15	13
	3.92	3.13	−57 −39 6	22

Height threshold: T = 3.85 (uncorrected p<0.001); extent threshold: k = 10 voxels.

Table 7

Significant results from the regression analysis performed on the map of functional connectivity with the left SMA at rest, considering deltaRATE, deltaTD and deltaITI as covariate.

Kinematic covariate	Cluster Size	Voxel T	Voxel Z	MNI Coordinate: x y z (mm)	Region
deltaRATE	46	7.96	4.61	30 57 −15	BA 11
		5.31	3.74	18 57 −12	BA 11
	84	6.76	4.26	39 −57 −57	Cerebellum (lobule VIII)
		6.68	4.24	33 −75 −48	Cerebellum (Crus II)
		6.14	4.06	24 −57 −57	Cerebellum (lobule VIII)
deltaTD	20	6.19	4.07	−12 −42 18	BA 29
		4.5	3.38	−9 −33 18	BA 23
deltaITI	17	5.87	3.96	−9 −6 15	Thalamus (anterior nucleus)
	23	5.75	3.91	3 −30 18	BA 23
		4.07	3.16	15 −33 12	Thalamus (Pulvinar)

BA = Brodmann area

Height threshold: T = 3.93 (uncorrected $p<0.001$); extent threshold: k = 10 voxels.

Table 8

Brain regions showing significant functional connectivity with the right SMA at rest.

Cluster Size	Voxel T	Voxel Z	MNI Coordinate: x y z (mm)	Region (Brodmann area)
5545	29.06	7.28	6 6 63	6
	17.59	6.37	0 −9 63	6
	14.18	5.95	12 18 57	6
412	11.84	5.58	−57 12 −3	22
	7.31	4.53	−57 −39 15	13
	6.84	4.38	−63 −45 27	40
52	8.21	4.79	−30 45 24	10

Height threshold: T = 3.85 (uncorrected p<0.001); extent threshold: k = 10 voxels.

Table 9

Significant results from the regression analysis performed on the map of functional connectivity with the right SMA at rest, considering deltaRATE, deltaTD and deltaITI as covariate.

Kinematic covariate	Cluster Size	Voxel T	Voxel Z	MNI Coordinate: x y z (mm)	Region (Brodmann area)
deltaRATE	54	6.62	4.22	33 60 -15	11
		4.97	3.6	33 51 -18	11
		4.96	3.59	24 51 -18	11
	64	6.33	4.12	66 -33 -24	20
		5.78	3.92	60 -21 -18	21
		5.73	3.9	69 -18 -27	20
deltaTD	No suprathreshold clusters				
deltaITI	No suprathreshold clusters				

Height threshold: T = 3.93 (uncorrected $p<0.001$); extent threshold: k = 10 voxels.